Changes in Model Lung Surfactant Monolayers Induced by Palmitic Acid

Frank Bringezu,[†] Junqi Ding,[†] Gerald Brezesinski,[‡] and Joseph A. Zasadzinski*,[†]

Department of Chemical Engineering, University of California, Santa Barbara, California 93106-5080, and Max Planck Institute of Colloids and Interfaces, Am Muehlenberg 1, D-14476 Golm/Potsdam, Germany

Received March 1, 2001. In Final Form: May 14, 2001

Pressure−area isotherms, Brewster angle microscopy, and grazing incidence X-ray diffraction measurements show that palmitic acid induces systematic changes in the physicochemical parameters and molecular organization of model lung surfactant lipid monolayers. Adding increasing fractions of palmitic acid (PA) to a 77/23 (wt/wt) mixture of dipalmitoylphosphatidylcholine (DPPC) and 1-palmitoyl-2-oleyl-phosphatidylglycerol (POPG) increased the solid-phase fraction of the monolayer as shown by pressure−area isotherms and fluorescence and Brewster angle microscopy. Grazing incidence X-ray diffraction showed that the palmitic acid interacted specifically with the DPPC fraction to form a mixed crystalline solid phase with a tilt angle that decreased in proportion to the fraction of palmitic acid. Increasing the PA content is roughly equivalent to increasing the surface pressure or decreasing the temperature of the DPPC/POPG monolayers. These results are important to the rational design of replacement lung surfactants for the treatment of respiratory distress syndrome.

Introduction

Lung surfactant is a complex mixture of lipids and proteins capable of forming a monolayer at the liquid−air interface in the lung alveoli. Proper lung function requires low surface tension provided by lung surfactants in order to minimize the work of breathing.[1−3] Although native surfactant is a complex, multicomponent, lipid−protein mixture,[3−5] key components have been identified that provide simplified model mixtures that mimic many of the features of native lung surfactants both in vitro and in vivo.[4−11] These are saturated dipalmitoylphosphatidylcholine (DPPC), unsaturated phophatidylglycerols (PG), and palmitic acid (PA) as the main lipid components[9,12,13] and the lung surfactant-specific apoproteins B and C.[14]

The multiple lipid and protein components are necessary because of the conflicting requirements of the surfactant monolayer. Rigid monolayers formed by DPPC alone can provide the necessary low surface tension on compression of the alveolar interface that accompanies exhalation. However, during the expansion that occurs on inhalation, the rapid spreading or adsorption of pure DPPC to cover the new interface is not possible.[15−17] On the other hand, fluid, fast-spreading unsaturated PGs cannot lower surface tension sufficiently.[18] A lack of effective surfactant, due to either immaturity in premature infants or various diseases in adults, can result in respiratory distress syndrome (RDS).[15,17,19,20] Typical treatment uses exogenous replacement surfactants, but supplies of human lung surfactant are limited, and therefore animal sources are most commonly used.[15,21−23] However, to minimize the risk of infection or immunological responses, synthetic surfactants designed for specific RDS applications are a major goal of research.[6−8,24,25] In addition, palmitic acid and DPPC are often added to extracted animal surfactants to improve surfactant performance.

Langmuir monolayers at the air−water interface provide accessible models for studies of lung surfactants and other amphiphilic molecules at the air−alveolus interface. Care is necessary to extrapolate Langmuir monolayer

* Corresponding author. Phone: 805-893-4769. Fax: 805-893-4731. E-mail: gorilla@engineering.ucsb.edu.

[†] University of California.

[‡] Max Planck Institute of Colloids and Interfaces.

(1) Schürch, S.; Goerke, J.; Clements, J. A. *Proc. Natl. Acad. Sci. U.S.A.* **1976**, *73*, 4698−4702.

(2) Schürch, S.; Goerke, J.; Clements, J. A. *Proc. Natl. Acad. Sci. U.S.A.* **1978**, *75*, 3417−3421.

(3) Goerke, J. *Biochim. Biophys. Acta* **1998**, *1408*, 79−89.

(4) Mizuno, K.; Ikegami, M.; Chen, C. M.; Ueda, T.; Jobe, A. H. *Pediatr. Res.* **1995**, *37*, 271−276.

(5) Pison, U.; Herold, R.; Schürch, S. *Colloids Surf.* **1996**, *114*, 165−184.

(6) Tanaka, Y.; Takei, T.; Aiba, T.; Masuda, K.; Kiuchi, A.; Fujiwara, T. *J. Lipid Res.* **1986**, *27*, 475−485.

(7) Cochrane, C. G.; Revak, S. D. *Science* **1991**, *254*, 566−568.

(8) Ding, J.; Takamoto, D.; von Nahmen, A.; Lipp, M. M.; Lee, K. Y. C.; Waring, A. J.; Zasadzinski, J. A. *Biophys. J.* **2001**, *80*, 2262−2272.

(9) Johansson, J.; Gustafsson, M.; Zaltash, S.; Robertson, B.; Curstedt, T. *Biol. Neonate* **1998**, *74*, 9−14.

(10) Lipp, M. M.; Lee, K. Y. C.; Takamoto, D. Y.; Zasadzinski, J. A.; Waring, A. J. *Phys. Rev. Lett.* **1998**, *81*, 1650−1653.

(11) Bernhard, W.; Mottaghian, J.; Gebert, A.; Rau, G. A.; von der Hardt, H.; Poets, C. F. *Am. J. Critical Care Medicine* **2000**, *162*, 1524−1533.

(12) Hawgood, S.; Derrick, M.; Poulain, F. *Biochim. Biophys. Acta* **1998**, *1408*, 150−160.

(13) Veldhuizen, R.; Nag, K.; Orgeig, S.; Possmayer, F. *Biochim. Biophys. Acta* **1998**, *1408*, 90−108.

(14) Johansson, J.; Curstedt, T.; Robertson, B. *Eur. Respir. J.* **1994**, *7*, 372−391.

(15) Poulain, F. R.; Clements, J. A. *West. J. Med.* **1995**, *162*, 43−50.

(16) Lee, K. Y. C.; Majewski, J.; von Nahmen, A.; Gopal, A.; Howes, P. B.; Kjaer, K.; Smith, G. S.; Zasadzinski, J. A. In preparation.

(17) Robertson, B.; Halliday, H. L. *Biochim. Biophys. Acta* **1998**, *1408*, 346−361.

(18) Takamoto, D. Y.; Lipp, M. M.; von Nahmen, A.; Lee, K. Y. C.; Waring, A. J.; Zasadzinski, J. A. *Biophys. J.*, in press.

(19) Clements, J. A. *Arch. Environ. Health* **1961**, *2*, 280.

(20) Clements, J. A. *Physiologist* **1962**, *5*, 11−28.

(21) Shapiro, D. L.; Notter, R. H. *Surfactant Replacement Therapy*; Liss: New York, 1989.

(22) Robertson, B. *Clin. Physiol.* **1983**, *3*, 97−110.

(23) Robertson, B. In *International symposium on surfactant replacement therapy*; Lachmann, B., Ed.; Springer-Verlag: Rotterdam, The Netherlands, 1987; pp 123−126.

(24) Phibbs, R. H.; Ballard, R. A.; Clements, J. A.; Heilbron, D. C.; Phibbs, C. S.; Schlueter, M. A.; Sniderman, S. H.; Tooley, W. H.; Wakely, A. *Pediatrics* **1991**, *88*, 1−9.

(25) Cochrane, C. G.; Revak, S. D. *Chest* **1994**, *105*, 57S−62S.

10.1021/la0103158 CCC: $20.00
Published on Web 00/00/0000 PAGE EST: 8

behavior to lung surfactant behavior in vivo, but general correlations between in vitro and in vivo behavior are starting to emerge.[3,8,10,26,27] The phase behavior of surfactants in two dimensions is determined by pressure−area isotherms. Additional information about the morphology of the monolayer domains is accessible by modern optical techniques such as fluorescence and Brewster angle microscopy.[28−31] Higher resolution information about the two-dimensional ordering on the angstrom scale is given by synchrotron grazing incidence X-ray diffraction (GIXD) measurements.[32−34] The combination of these methods gives a more complete picture of the relationship of monolayer molecular organization and structure to essential functions such as low minimum surface tension and rapid respreading.

DPPC by itself is capable of forming monolayers with minimum surface tensions near zero, which corresponds to a maximum surface pressure of about 70 mN/m. Over a range of surface pressures and temperatures between 20 and 37 °C, DPPC monolayers show coexistence between a disordered liquid expanded phase and ordered liquid condensed or solid phases.[28] In the condensed phase domains, the hydrocarbon chains exhibit an oblique lattice with molecules tilted in a nonsymmetry direction.[35] On compression, the tilt angle is decreased, but tilts of more than 25° are still observed at lateral pressures above 40 mN/m.[35] The chain tilt can be explained by the large area required for the well-hydrated polar headgroup of DPPC relative to the smaller area required for the hydrocarbon chain region. The area requirements determined by the molecular shape can be reconciled by tilting the chains; the chains tilt until the projected area of the hydrocarbon chains in the plane normal to monolayer (i.e., the plane of the water surface) is increased to match that of the headgroups.[36] Unsaturated phosphatidylglycerols form only unstructured liquid expanded phases over their entire range of surface pressure at physiological temperatures.[18]

Palmitic acid is a common additive to replacement lung surfactants and improves certain surface properties as shown in vitro[5,6,15,17,37] and in clinically used replacement surfactants in vivo.[3,4] However, PA's function in the monolayer and its interaction with the other components of the monolayer are not particularly well understood.[38] Long-chain saturated fatty acids such as PA exhibit condensed phase monolayers over a wide temperature range. Extensive X-ray and microscopy revealed a generic phase diagram for fatty acid monolayers.[34] For palmitic acid, the molecular order is crystalline with tilted chains, generally in a centered rectangular unit cell. Both the extent of chain tilt and the tilt direction are functions of the lateral pressure and the temperature. With increasing surface pressure, the tilt direction changes from nearest neighbor (NN, along the short axis of the unit cell) to next nearest neighbor (NNN, along the long axis of the unit cell) and the tilt angle decreases.

However, recent work has shown that mixtures of PA and DPPC interact specifically in monolayers to produce new crystalline packings different than those of either pure lipid.[16] Adding PA to DPPC monolayers acts to condense the monolayers, leading to a greater fraction of solid condensed phase at a given surface pressure and temperature. At a given surface pressure, increasing the PA fraction in the DPPC monolayer decreases the molecular tilt; at about a 1:1 mole ratio, the tilt has decreased to zero. In this paper, we show that a similar increase in the solid phase fraction and decrease in molecular tilt occurs in a more complex lipid mixture of DPPC, PA, and 1-palmitoyl-2-oleyl-phosphatidylglycerol (POPG) that is a reasonable model of the lipids in lung surfactants. The POPG provides a noncondensable fluid phase at all surface pressures and temperatures. We present isotherm measurements, Brewster angle microscopy results, and grazing incidence X-ray diffraction measurements to show that PA induces a similar systematic increase in the fraction of condensed phase and a similar decrease in molecular tilt in those condensed phases in the mixed model systems. These observations suggest that PA, when added to animal surfactant extracts rich in DPPC, likely acts to increase the solid-phase fractions in those monolayers and increases the rigidity of the surfactant monolayer, especially at low surface tensions.

Experimental Section

Materials. 1,2-Dipalmitoyl-*sn*-glycero-3-phosphatidylcholine (DPPC) and 1-palmitoyl-2-oleyl-*sn*-glycero-3-phosphatidylglycerol (POPG) were purchased from Avanti Polar Lipids (Alabaster, AL; purity > 99%). Palmitic acid was obtained from Sigma Chemical Co. (St. Louis, MO; purity > 99%). All lipid samples were used without further purification. Water was prepared using a Millipore Milli-Q system and had a resistivity of > 18 MΩ cm^{-1}.

Methods. The monolayer experiments have been performed using a home-built Langmuir trough equipped with a Wilhelmy-type pressure-measuring device and two computer-controlled barriers that provided a symmetric compression. A stock spreading solution of a 77/23 wt/wt mixture of DPPC/POPG (about 1 mg/mL) was prepared using pure chloroform as solvent. Various amounts of palmitic acid were added to this stock solution and then spread onto pure water a pure water subphase to form monolayers. The following mixing ratios (DPPC/POPG/PA, by weight (by mole)) were examined: **M1**, 77/23/0 (78/22/0); **M2**, 73/22/5 (67/19/13); **M3**, 69.5/20.5/10 (59/17/24); **M4**, 62/18/20 (45/13/42); **M5**, 46/14/40 (26/8/66); **M6**, 31/9/60 (15/4/81); **M7**, 15.5/4.5/80 (6/2/92).

For the BAM experiments, an argon ion laser was used as light source. A rotatable mirror and a polarizer (Melles-Griot, Sunnyvale, CA) placed between laser and trough provided p-polarized light at the Brewster angle (approximately 53° from vertical for a pure water surface). A simple lens (Melles-Griot) or a long focal microscopic objective (Nikon) was used to collect the reflected light. An additional polarizer was used as analyzer in order to improve the contrast of the final images, which are detected by a Sony CCD camera (model XC-75). The images were recorded using a JVC super VHS VCR (Elmwood Park, NJ) and processed using a custom computerized data acquisition system.

For fluorescence imaging, a Nikon Optiphot with the stage removed is positioned above the trough. A 40× power long working distance objective designed for use with fluorescence systems is used. The trough is mounted on a motorized *xyz* translation stage: the *z* axis is used for focusing, and the *x* and *y* axes are used to scan over different regions. A 100 W high-pressure mercury lamp was used for excitation. A dichroic mirror/barrier filter assembly is used to direct the excitation light onto the monolayer (with a normal angle of incidence) and to filter the

(26) Johansson, J.; Curstedt, T. *Eur. J. Biochem.* **1997**, *244*, 675−689.
(27) Schürch, S.; Green, F. H. Y.; Bachofen, H. *Biochim. Biophys. Acta* **1998**, *1408*, 180−202.
(28) McConnell, H. *Annu. Rev. Phys. Chem.* **1991**, *42*, 171−195.
(29) Möbius, D.; Möhwald, H. *Adv. Mater.* **1991**, *3*, 19−24.
(30) Hénon, S.; Meunier, J. *Rev. Sci. Instrum.* **1991**, *62*, 963−969.
(31) Lipp, M. M.; Lee, K. Y. C.; Zasadzinski, J. A.; Waring, A. J. *Rev. Sci. Instrum.* **1997**, *68*, 2574−2582.
(32) Als-Nielsen, J.; Jacquemain, D.; Kjaer, K.; Leveiller, F.; Lahav, M.; Leiserowitz, L. *Phys. Rep.* **1994**, *246*, 251−313.
(33) Kjaer, K. *Physica A* **1994**, *198*, 100−109.
(34) Kaganer, V. M.; Mohwald, H.; Dutta, P. *Rev. Mod. Phys.* **1999**, *71*, 779−819.
(35) Brezesinski, G.; Dietrich, A.; Struth, B.; Boehm, C.; Bouwman, W. G.; Kjaer, K.; Moehwald, H. *Chem. Phys. Lipids* **1995**, *79*, 145−157.
(36) Dahmen-Levison, U.; Brezesinski, G.; Mohwald, H. *Thin Solid Films* **1998**, *327*, 616−620.
(37) Tanaka, Y.; Tsunetomo, T.; Kanazawa, Y. *Chem. Pharm. Bull.* **1983**, *31*, 4100−4109.
(38) Cockshutt, A. M.; Absolom, D. R.; Possmayer, F. *Biochim. Biophys. Acta* **1991**, *1085*, 248−256.

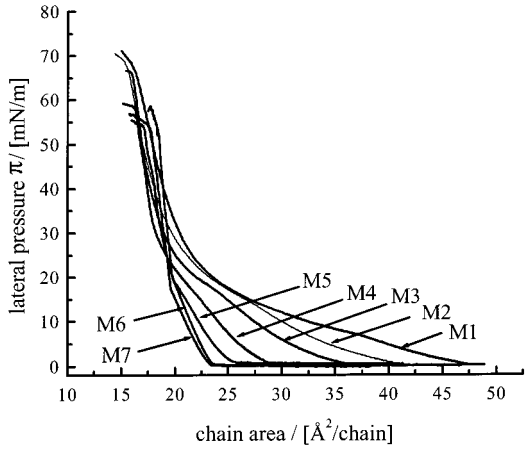

Figure 1. $\pi-$A isotherms of surfactant mixtures with different concentrations of PA. The DPPC/POPG ratio is constant (77/23, w/w). The addition of PA results in a systematic variation of the lipid composition. DPPC/POPG/PA (w/w/w): **M1**, 77/23/0; **M2**, 73/22/5; **M3**, 69.5/20.5/10; **M4**, 62/18/20; **M5**, 46/14/40; **M6**, 31/9/60; **M7**, 15.5/4.5/80. The chain area is given considering two chains from DPPC and POPG and a single chain from PA.

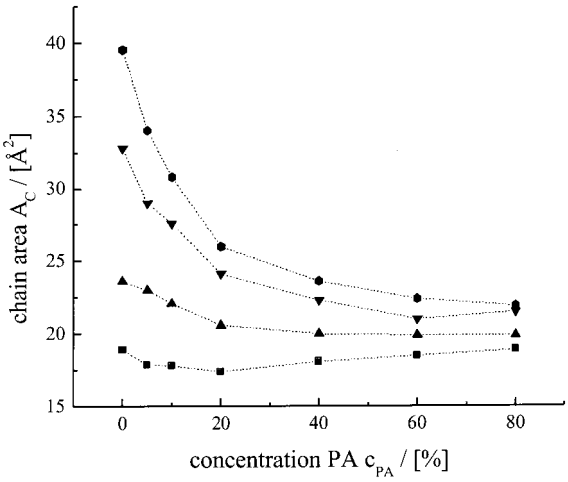

Figure 2. Area composition plot of the mixtures of DPPC, POPG, and PA at different pressures. All mixtures contain a 77/23 (w/w) ratio of DPPC to POPG. The weight percentage of PA to total surfactant increases from 0 to 80% (w/w) between mixture **M1** and **M7** (**M1**, 0% PA; **M2**, 5% PA; **M3**, 10% PA; **M4**, 20% PA; **M5**, 40% PA; **M6**, 60% PA; **M7**, 80% PA). The curves show the area values per hydrocarbon chain extracted from the isotherms at different pressures: 5 mN/m (●), 10 mN/m (▼), 20 mN/m (▲), and 40 mN/m (■).

emitted fluorescence. The emitted fluorescence is collected by the objective and detected via a silicon intensified target (SIT) camera. Images are recorded by a JVC super VHS VCR and digitized via a Scion frame grabber. The resulting digitized images are processed and analyzed following a custom-designed protocol.[31] The lipid mixtures are doped with 0.5 mol % of the fluorescent lipid Texas Red-DHPE (Molecular Probes) for fluorescence imaging.

GIXD measurements were performed at 20 °C using the liquid surface diffractometer on the beam line BW1 at HASYLAB, DESY, Hamburg, Germany. The Synchrotron beam was made monochromatic by a beryllium (002) crystal. Experiments were performed at an angle of incidence of $0.85\alpha_c$ (α_c is the critical angle for total external reflection). A linear position sensitive detector (PSD) (OED-100-M, Braun, Garching, Germany) with a vertical acceptance $0 < Q_Z < 1.27$ Å^{-1} was used for recording the diffracted intensity as a function of both the vertical (Q_z) and the horizontal (Q_{xy}) scattering vector components. The horizontal resolution of $Q_{XY} = 0.0075$ Å^{-1} was determined by a Soller collimator mounted in front of the PSD. The analysis of the in-plane diffraction data yields lattice spacings according to $d_{hk} = 2\pi/Q_{xy}^{hk}$. From the maximum position of the in-plane scattering vector components, it is possible to derive information about the tilt angle and tilted direction. The principles of GIXD for the study of two-dimensional crystalline films at the air−liquid interface are summarized in recent reviews.[32,34,39]

Results

Figure 1 displays the pressure−area isotherms for different lipid mixtures; the ratio of DPPC to POPG was held constant, and the weight fraction of PA was changed from 0 to 80%. The area is scaled per hydrocarbon chain (one per PA and two per DPPC or POPG) instead of area per molecule that is typically used. Without PA (**M1**), the isotherm shows "lift-off" or the first increase in the surface pressure at 47 Å^2/chain followed by a smeared-out plateau between 37 and 25 Å^2/chain. In the high-pressure region above 30 mN/m, the surface pressure is an almost linear function of A_C up to a collapse pressure of about 65−70 mN/m, indicating condensed phases of low compressibility. On going from **M1** to **M6**, the addition of PA changes the isotherms drastically, shifting the lift-off pressure toward lower areas per chain. Increasing the PA fractions up to 40% systematically lowers the collapse pressures (π_{col}) (70 mN/m, 0% PA; 67 mN/m, 10% PA; 58 mN/m, 20 PA %); above 40% PA, the values level off at about 55 ± 2 mN/m. The slope of the isotherm, which is proportional to the compressibility of the monolayer, also systematically increases with increasing PA fraction. The mixture **M3** shows a shift of the plateau region toward higher pressures (∼17 mN/m), corresponding to an increase of the transition temperature of the monolayer. At higher PA contents, the plateau disappears completely, and for **M4**−**M7**, a discontinuous change in the slope of the isotherms at about 15−20 mN/m indicates a second-order phase transition at surface pressures similar to those for a pure palmitic acid monolayer. This could be interpreted in terms of a separation of the condensed monolayer into pure PA domains and a second condensed phase with PA/DPPC/POPG at a fixed mixing ratio.

Figure 2 displays the area per chain versus composition plots for all mixtures investigated. The data have been extracted from the isotherms at different lateral pressures. On going from **M1** to **M7** at 5 mN/m, increasing the PA fraction shifts the area per chain from 39 Å^2/chain (**M1**) to 22 Å^2/chain (**M7**). With increasing pressure, this drop diminishes continuously leading to almost constant values for the areas per chain of about 18 Å^2 at 40 mN/m. Adding PA at constant surface pressure leads to a more condensed monolayer packing at low surface pressures.

Visualizing the monolayers using Brewster angle microscopy (BAM) shows the variation in morphology that accompanies the changes in the isotherms (Figure 3). The contrast in BAM images is due to local differences in the monolayer refractive index caused by differences in local molecular density or packing. At 20 °C and a surface pressure of 5 mN/m, **M1** (77/23/0 DPPC/POPG/PA) appears dark gray, with no contrast, indicating a uniform liquid expanded phase (see Figure 3). At 10 mN/m, the monolayer shows bright condensed phase domains with an average size of 20 μm in a continuous background of darker liquid expanded phase. At 20 mN/m, the size of the bright condensed phase domains increases to about 25 μm. Further increases in the surface pressure are accompanied by a decrease in contrast, indicating an

(39) Jacquemain, D.; Leveiller, F.; Weinbach, S.; Lahav, M.; Leiserowitz, L.; Kjaer, K.; Als-Nielsen, J. *J. Am. Chem. Soc.* **1991**, *113*, 7684.

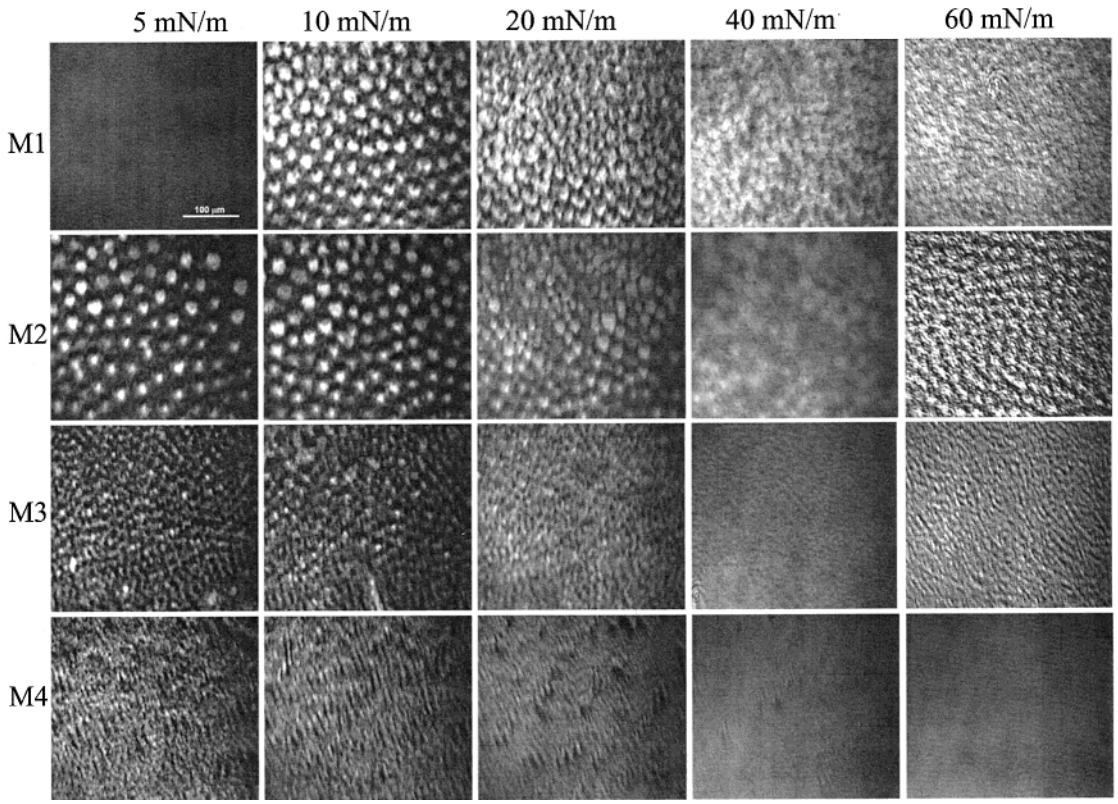

Figure 3. Brewster angle micrographs of surfactant mixtures **M1**−**M4** (**M1**, 0% PA; **M2**, 5% PA; **M3**, 10% PA; **M4**, 20% PA). From top to bottom, each row corresponds to a single mixture; the columns give the surface pressure at which the micrograph was recorded. Contrast in the micrographs arises from coexistence of fluid (dark areas) to condensed domains (bright areas). By rotation of the analyzer in the Brewster angle microscope, the bright domains can change to dark domains, which indicates the monolayer is tilted. As the percentage of PA is increased at a given surface pressure (e.g., 5 mN/m), the fraction of monolayer that is condensed also increased. At a certain pressure, the contrast was lost and the rotating analyzer cannot create dark−bright change anymore, which shows the monolayer is untilted. Similarly, as the surface pressure imposed on a given surfactant mixture is increased, the fraction of the monolayer surface occupied by condensed domains increases. With increasing PA concentration, the untilted pressure lowers. The scaling of the images is given by the bar shown for **M1** at 5 mN/m which represents 100 μm.

almost complete conversion to a condensed phase with uniform molecular orientation. At the highest pressure of 60 mN/m, the image shows an increase in contrast consistent with a distribution of small domains. However, the resolution of the BAM is not sufficient to resolve the shape of the domains or their exact size.

Adding PA shifts the two-phase coexistence region toward lower pressures, leading to circular condensed phase domains in sample **M2** (DPPC/POPG/PA 73/22/5) at 5 mN/m. At higher PA fractions, only the condensed phase with small domains (**M3**, 69.5/20.5/10; **M4**, 62/18/20) is observed even at 5 mN/m. The appearance of samples **M3** and **M4** at low pressures is similar to that of the clinical surfactant Survanta, which contains added palmitic acid.[8] The transition toward a lack of contrast indicative of a uniform orientation occurs at lower pressures for the samples with a higher PA content. The BAM images are consistent with the isotherms and show that PA induces a condensation of the monolayer at all surface pressures.

Higher resolution images of samples **M1** (77/23/0 DPPC/POPG/PA) and **M4** (62/18/20 DPPC/POPG/PA) were obtained using fluorescence microscopy (Figure 4). At 5 mN/m (Figure 4A), **M1** shows a uniform liquid expanded phase, consistent with the BAM images (Figure 3). At 10 mN/m (Figure 4B), first condensed domains appear. With increasing pressure at 20 mN/m (Figure 4C), sample **M1** shows characteristic chiral liquid condensed domain shapes (dark) similar to those of pure DPPC[28] in a continuous phase of liquid expanded phase (bright). The image contrast is reversed between the BAM and the fluorescence images: in BAM, the condensed phase domains are bright and the liquid phases are dark, whereas in fluorescence images, the condensed phases are dark and the liquid phases are bright. Finally, at 40 mN/m, the image of sample **M1** shows primarily condensed phase domains separated by a smaller fraction of the liquid expanded phase. At a higher PA content of 20% in sample **M4**, the images appear darker in the whole pressure region. At low lateral pressures, a continuous dark phase is observed. Increasing pressure results in a transition at ~8 mN/m. Above this pressure, the monolayer shows dark condensed domains in a continuous liquid expanded matrix (bright, see Figure 4B right) as observed at lower PA concentrations. At higher pressures above 20 mN/m, the image is dominated by the dark condensed domains showing circular shape.

To quantify the condensing effect of palmitic acid, GIXD was used to determine the in-plane structures in the condensed phase portion of the monolayers on the angstrom scale. GIXD only is sensitive to the ordered phases of the monolayer; the fluid phases only contribute to the background. Figure 5 shows selected contour plots of the corrected X-ray diffraction intensities as a function of the in-plane scattering vector component Q_{XY} and the out-of-plane scattering vector component Q_Z for the mixtures **M1** (77/23/0 DPPC/POPG/PA), **M3** (69.5/20.5/10), and **M4** (62/18/20), respectively.

Starting at low pressures, the system **M1** exhibits three low-order diffraction peaks up to 35 mN/m (see Figure 5A). Such an intensity profile is characteristic for an

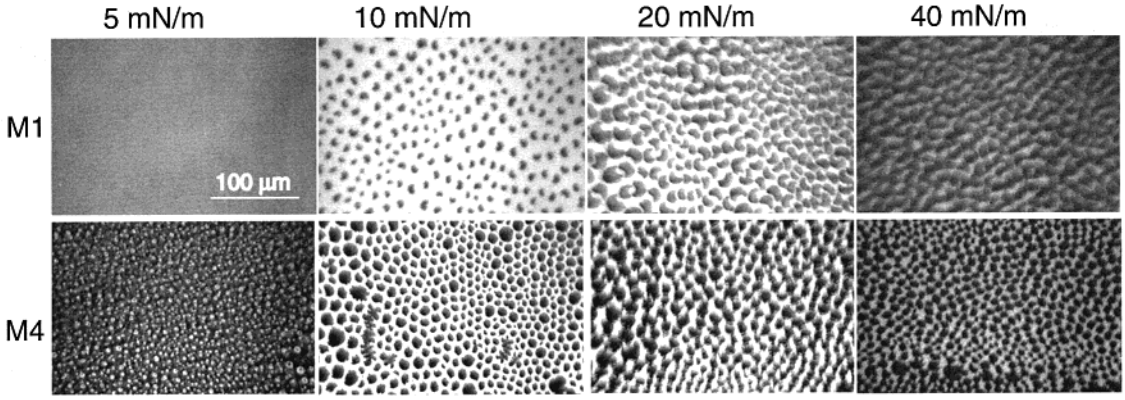

Figure 4. Fluorescence images of surfactant mixtures of DPPC, POPG, and PA: **M1** (top) and **M4** (bottom). Both systems contain 0.5 mol % DHPE Texas Red as dye. The images were taken at 20 °C on a pure water subphase at different surface pressures indicated. The bar shown for **M1** at 5 mN/m represents 100 μm.

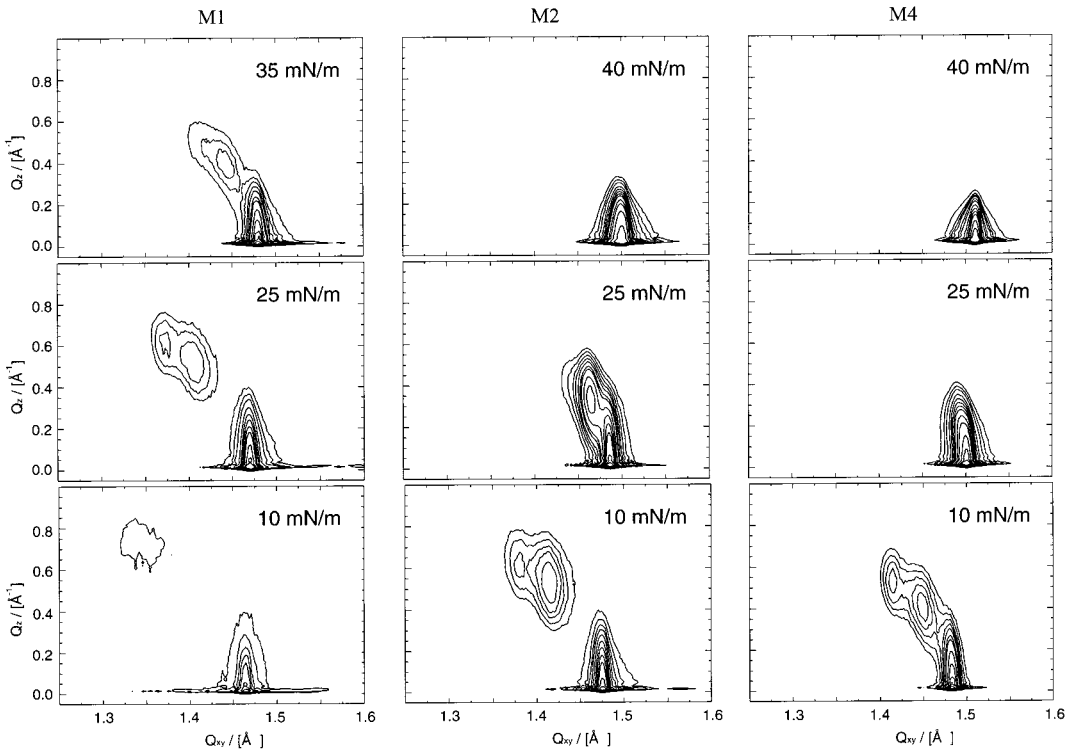

Figure 5. Contour plots of the corrected X-ray intensities versus in-plane scattering vector component Q_{XY} and out-of-plane scattering vector component Q_Z of the scattering vector **Q** for surfactant mixtures **M1**, **M2**, and **M4** at 20 °C and different pressures indicated.

oblique chain lattice without mirror symmetry.[34] The maxima of the Bragg rods are located above the horizon; thus, the chains are tilted from the perpendicular to the surface. The tilt angle is 32 ± 1°, and the tilt azimuth is in a nonsymmetry direction (neither NN nor NNN). The fitted Bragg peak positions lead to spacings of 4.29, 4.64, and 4.75 Å. Increasing lateral pressure results in a shift to smaller lattice spacings and decreases the chain tilt. Between 35 and 50 mN/m, a phase transition occurs. At 50 mN/m, only two diffraction peaks are observed, one at $Q_Z = 0$ Å^{-1} and a second at higher Q_Z values (see Figure 6). Such a distribution is typically observed for tilted chains in a centered rectangular lattice with a tilt azimuth in the direction of the NN.[34] Figure 6 shows the fitted peak positions at 50 mN/m that result in spacings of 4.28 Å (d_{11}) and 4.25 Å (d_{02}) and a residual chain tilt of (10 ± 1)°. Both the decrease in spacings and the chain tilt cause a decrease in the projected area per chain in the plane of the monolayer, A_{XY}, from 24 Å^2 (10 mN/m) to 20.8 Å^2 (50 mN/m).

On increasing the PA fraction from 0 to 10% (sample **M3**) at 10 mN/m, the general features of the diffraction pattern are not changed; however, the peak positions are shifted leading to a lower molecular tilt of 26 ± 1° and smaller lattice spacings, consistent with a condensing effect of PA. The lattice parameters decrease about 4% in the (01) and (10) directions but only 0.7% in the (11) direction. On increasing the surface pressure to 40 mN/m, the in-plane components Q_{XY} coincide, indicating hexagonal symmetry; however, intensity is observed up to high Q_Z values suggesting NN tilted chains with a tilt of about 7 ± 1°.[34] A single reflection of vertically oriented chains at a spacing of 4.17 Å is observed at 50 mN/m.

At an increased PA concentration of 20% (sample **M4**), the phase sequence remains unchanged; however, the phase transition pressures shift to lower values. Three

Table 1. Fitted Peak Parameters of the Three Low-Order Reflections of the Diffracted X-ray Intensities Given in Terms of the Horizontal (In-Plane, Q_{XY}) and Vertical (Out-of-Plane, Q_Z) Scattering Vector Components

		(1 ± 1) [Å^{-1}]				(01) [Å^{-1}]				(10) [Å^{-1}]			
system	π [mN/m]	Q_{xy}	ΔQ_{xy}	Q_z	ΔQ_z	Q_{xy}	ΔQ_{xy}	Q_z	ΔQ_z	Q_{xy}	ΔQ_{xy}	Q_z	ΔQ_z
M1	10	1.464	0.014	0.07	0.27	1.355	0.051	0.66	0.25	1.323	0.050	0.72	0.27
	25	1.470	0.014	0.08	0.28	1.405	0.049	0.53	0.29	1.370	0.036	0.62	0.28
	35	1.479	0.020	0.08	0.30	1.439	0.045	0.40	0.30	1.409	0.037	0.48	0.30
	50	1.486	0.019	0	0.30	1.477	0.037	0.23	0.30	1.477	0.037	0.23	0.30
M3	10	1.475	0.013	0.1	0.28	1.414	0.034	0.53	0.28	1.378	0.027	0.63	0.28
	25	1.486	0.017	0.07	0.30	1.462	0.024	0.38	0.29	1.435	0.025	0.45	0.29
	40	1.499	0.018	0	0.32	1.499	0.018	0.15	0.28	1.499	0.018	0.15	0.28
	50	1.506	0.020	0	0.24	1.506	0.020	0	0.24	1.506	0.020	0	0.24
M4	10	1.483	0.016	0.11	0.29	1.448	0.036	0.41	0.29	1.414	0.029	0.53	0.28
	25	1.499	0.017	0	0.28	1.496	0.021	0.20	0.28	1.496	0.021	0.20	0.28
	40	1.510	0.014	0	0.24	1.510	0.014	0	0.24	1.510	0.014	0	0.24
	50	1.512	0.014	0	0.23	1.512	0.014	0	0.23	1.512	0.014	0	0.23

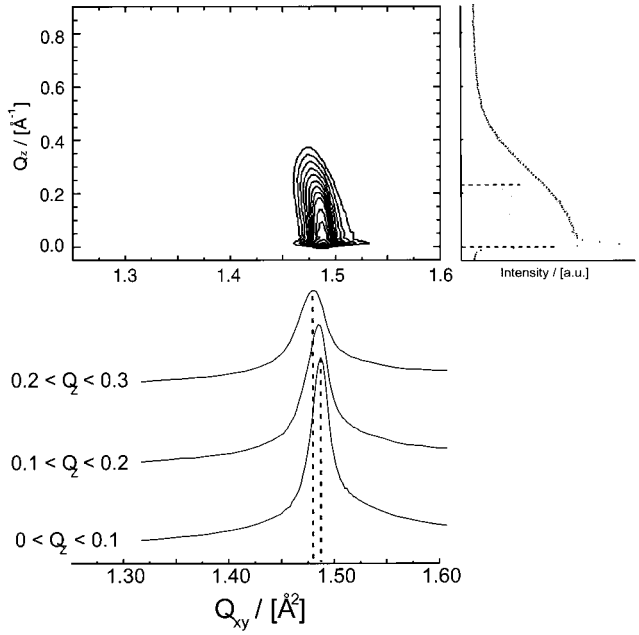

Figure 6. Intensity contour plot of the corrected X-ray intensities for sample **M1** obtained at 20 °C and 50 mN/m. Over certain Q_Z ranges, summarized intensities are plotted below. The fitted peak positions are marked in the plot. The summarized intensities between 1.46 Å^{-1} < Q_{XY} < 1.51 Å^{-1} are given right of the contour. The fit with two Gaussian peaks and the peak maxima are shown in the plot. From the peak positions, the tilt angle of the hydrocarbon chains of 10 ± 1° was calculated.

peaks of an oblique chain lattice could only be resolved at 10 mN/m for the 20% PA concentration. The centered rectangular symmetry is obtained at 25 mN/m, and at a surface pressure of 40 mN/m, hexagonal symmetry is found. At 50 mN/m, sample **M4** exhibits the smallest lattice spacing of 4.15 Å observed in the systems. The fitted peak positions are given in Table 1.

Discussion

All components used in our studies are major constituents of the pulmonary surfactants in the lungs that are responsible for the adjustment of the physicochemical properties of the alveolar interfaces, especially the surface tension.[3] Native pulmonary surfactants are much more complex mixtures, but the lipids studied in this paper are representative of the lipid classes in native surfactant and are consistent with those used in replacement surfactants.[11] These model systems are amenable to the systematic study of lipid−lipid interactions that play a major role in the regulation process in natural and replacement lung surfactants.[3,6,13,15,17] Single-component DPPC, PA, or POPG lipid monolayers show quite different phase behavior than that observed here in mixed monolayers. By varying fatty acid fraction, we have shown that PA has a strong influence on the phase behavior of mixed DPPC/POPG monolayers that would not be expected from the pure-component phase diagrams. As our model monolayers are similar to those in native and replacement surfactants, at least in lipid class (phosphatidylcholine and phosphatidylglycerol, saturated and unsaturated), it is likely that PA has a similar condensing effect in those monolayers as well.

The pressure−area isotherms and BAM images show that the addition of PA to the model system initially shifts the first-order transition from liquid expanded (LE) to liquid condensed (LC) phases to lower pressures. For 20% and higher PA concentrations (samples **M4**−**M7**), no LE phase is observed; hence, these monolayers are below their triple point temperatures.[18] Adding PA lowers the effective temperature of the mixed monolayer, leading to more condensed phases at a given surface pressure. This condensing effect is also observed in binary mixtures of DPPC with PA and DPPC with hexadecanol.[16] In crystalline L_2'' and C_S phases of single-chain fatty acids, area values of about 19 Å^2 are found.[34,40] The isotherm measurements show values of approximately 18 Å^2/chain for the mixtures investigated. On the other hand, double-chain lipids such as DPPC and the expanded unsaturated POPG exhibit A_{XY} values above 19 Å^2. Therefore, at pressures above 40 mN/m a squeeze-out of expanded components that are not incorporated in the condensed lattice must be assumed.

The major components of the mixtures investigated are DPPC and PA. Model studies on lipid−water dispersions have shown that fatty acids drastically affect both the structure and the thermotropic phase behavior of lipid bilayers.[41−43] Increasing PA content up to 5% suppresses the formation of the DPPC subgel phase at 17 °C, and higher PA concentrations lead to the formation of a new gel phase resulting from cocrystallization in the ratio of 1 DPPC/2 palmitic acid molecules. In the monolayer experiments, the mixture **M4** with a DPPC/PA molar ratio of about 1:1 shows at low lateral pressures a continuous dark phase, which is not observed at low PA content (**M1**−**M3**). This could be an indication for a formation of a complex at a specific lipid−fatty acid ratio that forms the condensed matrix. Assuming a ratio of 1:2, the bright

(40) Peterson, I. R.; Brzezinski, V.; Kenn, R. M.; Steitz, R. *Langmuir* **1992**, *8*, 2995−3002.
(41) Marsh, D.; Seddon, J. M. *Biochim. Biophys. Acta* **1982**, *690*, 117−123.
(42) Koynova, R. D.; Tenchov, B. G.; Quinn, P. J.; Laggner, P. *Chem. Phys. Lipids* **1988**, *48*, 205−214.
(43) Katsaras, J.; Stinson, R. H. *Biophys. J.* **1990**, *57*, 649−655.

domains in the dark matrix (Figure 4) must then consist of the remaining DPPC−POPG molecules. This idea is supported by the area fraction of the dark phase (Figure 4, **M4** at 5 mN/m) of about 60% that corresponds well to the molar ratios of the 1:2 DPPC−PA complex and the remaining lipid components.

Lung surfactant function in vivo is generally correlated with the minimum surface tension and adsorption and respreading behavior of the monolayer in vitro.[5,11,38] Adding PA lowers the collapse pressure of the film and hence increases the minimum surface tension. For the DPPC/POPG mixture, **M1**, a collapse pressure of 70 mN/m was obtained, while on addition of PA the values drop (**M2**, 66 mN/m) and level off at concentrations above 40% PA at about 55 ± 2 mN/m. As increasing the PA content decreases the collapse pressure, it is more likely that the change in the monolayer morphology and local molecular packing that PA induces are responsible for the improved performance of lung surfactant replacements such as Survanta, an animal extract surfactant to which PA is added.[6] At high PA concentrations, the isotherms display a kink that could be interpreted as a second-order transition between two condensed phases that is also observed in the case of the pure fatty acid. The question arises whether this could be an indication of a phase separation of a PA-enriched phase from a second, more DPPC-enriched phase.

GIXD measurements have shown that the structure of the condensed phases changes systematically with PA content. All mixtures investigated exhibit oblique tilted phases for sufficiently low surface pressures. Increasing the surface pressure decreases the tilt and leads to phase transitions that change the symmetry of the lattice, leading finally to hexagonal phases of vertically oriented chains. Despite the overall similarities, there are remarkable differences in the monolayer depending on the PA concentration. Increasing the PA fraction leads to lower tilt angles at all surface pressures. Zero tilt occurs only after addition of PA (the DPPC/POPG mixtures remained tilted at the highest surface pressures), and higher PA concentration shifts the NN−hexagonal transition toward lower pressure.

At these temperatures in condensed phases, the shift in the projected area per chain in the plane of the monolayer, A_{XY}, is due to a change in the tilt angle and not to any variation in the cross-sectional area of the chain A_0.[34] The tilt angle, t, is therefore related to the area per chain according to $\cos(t) = A_0/A_{XY}$. In the condensed phases, the pressure−area isotherms are essentially straight lines so that the A_{XY} values can be described as almost linear functions of the lateral pressure: $A_{XY} = K_1 - K_2\pi$. Therefore, 1/cos(t) should be linearly dependent on π. The transition pressure for packing with upright orientation of the chains can be derived by extrapolation to zero tilt (see Figure 7). The mixture **M1** shows the transition toward upright orientation at about 53 mN/m. Adding PA to the system shifts this pressure almost linearly with PA concentration (**M3**, 40 mN/m; **M4**, 28 mN/m) to lower values.

In a comparison of all three mixtures, mixture **M1** containing only DPPC and POPG shows the largest tilt (32 ± 1°). Pure DPPC monolayers exhibit an oblique chain lattice that is only slightly distorted from centered rectangular symmetry. The chains in the pure DPPC monolayer exhibit a tilt of 37°, which can be explained by a mismatch in the space requirements between the large hydrated PC headgroup and the two saturated alkane chains connected to the glycerol backbone.[16,35] It has been shown that this area mismatch can be compensated by

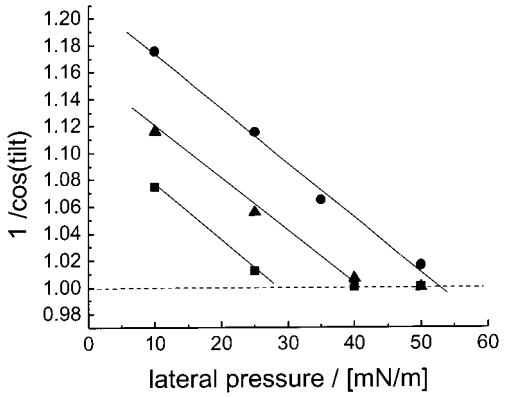

Figure 7. 1/cos(t) as a function of the lateral pressure π for mixture **M1** (●), M2 (■), and **M4** (▲). t is the tilt angle of the molecules to normal. From the extrapolation toward 1/cos(t) = 1, the transition pressure toward upright orientation was obtained.

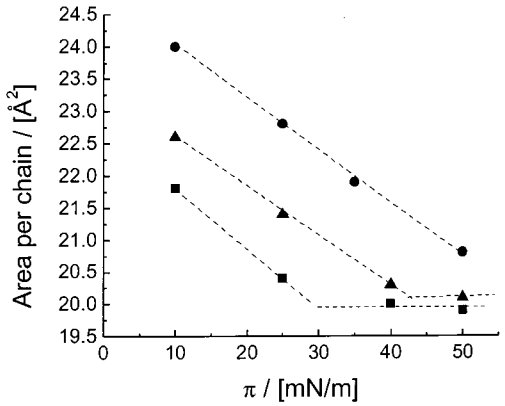

Figure 8. Projected area A_{xy} per hydrocarbon chain in the condensed lattice as a function of the lateral pressure π for mixtures **M1** (●), **M2** (■), and **M4** (▲) as determined by GIDX measurements.

incorporation of alkanes into the DPPC chain lattice, leading to decreased tilt angles.[44] Exchanging the smaller phosphatidylethanolamine headgroup results in vertically oriented chains at high pressures, and hence, no incorporation of alkanes is observed.[44,45] The addition of POPG results in a decreased chain tilt by about 5°, but the vertical orientation of the molecules observed after alkane incorporation could not be achieved. Moreover, for mixture **M4**, three distinct peaks are clearly separated at low surface pressure (see Figure 5A, bottom); thus, the distortion from centered rectangular symmetry is increased by the presence of POPG in the mixture.

Figure 8 shows the projected area per chain A_{XY} obtained in GIXD experiments. Without PA, the chain area of 24 Å^2 decreases linearly with increasing surface pressure. Addition of PA results in a decrease in A_{XY} at a given surface pressure, and the curves level off at a limiting area of about 20−20.5 Å^2 at high surface pressure. This limiting area is similar to those reported for single-component fatty acid monolayers in hexagonally packed, vertically oriented phases.[34] Additional information is given on comparing the area values obtained from GIXD experiments, A_{XY}, with the area per chain, A_C, extracted from the pressure−area isotherms (see Table 2). Since only the condensed part of the monolayer contributes to the A_{XY} measured by GIXD, there must be an additional

(44) Brezesinski, G.; Thoma, M.; Struth, B.; Mohwald, H. *J. Phys. Chem.* **1996**, *100*, 3126−3130.
(45) Thoma, M.; Möhwald, H. *Colloids Surf., A* **1995**, *95*, 193−200.

Table 2. Area Values Calculated from Peak Positions Obtained in GIXD Measurements (A_{XY}) and Extracted from the Pressure−Area Isotherm Experiments (A_C)[a]

system	A_{XY}/[Å^2]	A_C/[Å^2]	ζ_{XY}/[%]	ζ_C/[%]
M1	24.0	32.5	74	71
M3	21.4	27.5	78	83
M4	21.8	24.0	91	87

[a] The values are obtained at a lateral pressure of 10 mN/m. From the area difference, the portion of the crystalline area fraction (ζ_{XY}) of the layer has been calculated. The composition of the mixture gives the proportion of the condensed lipids (ζ_C).

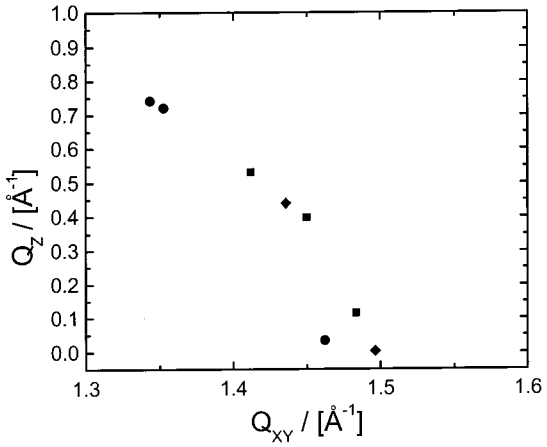

Figure 9. Fitted peak positions of the X-ray diffraction signals as a function of the in-plane scattering vector component Q_{XY} and out-of-plane scattering vector component Q_Z obtained for DPPC (●), PA (♦), and the mixture **M4** (■) at 10 mN/m and 20 °C. The different peak positions found for all samples indicate that M4 exhibits a mixture in the condensed state rather than a demixed system of pure DPPC or PA.

contribution to the area per chain due to either lattice defects or, as shown by the BAM images, a fluid phase of POPG. This explains the difference found on comparing A_C with A_{XY}. From these values, the area fraction covered by the crystalline chains ζ_{XY} can be deduced. This value is close to the molecular fraction of DPPC and PA given by the mixing ratio. It seems most probable that the crystalline structures consist of essentially all of the DPPC and PA in the monolayer while nearly pure POPG forms the liquid expanded matrix seen in the BAM images. However, it must be noted that the remaining area fraction of the expanded phase should exhibit higher area values because the more flexible chains in the LE phase require more space. Consequently, an incorporation of some POPG molecules in the crystalline structure has to be assumed, consistent with the change in the DPPC lattice in sample **M1**. It is also important to note that at higher surface pressures, A_{XY} values are larger than the corresponding A_C values. This is only possible if there was a loss or squeeze-out of some fraction of the liquid expanded matrix on going to higher pressures. This squeeze-out has been observed previously for mixtures of solid phase and fluid phase lipids at high surface pressures.[8,10,18]

To prove miscibility of PA and DPPC in the condensed phase domains, Figure 9 shows the fitted peak positions of the intensity distribution of the diffraction signal for DPPC, PA, and the mixture **M4** obtained at low lateral pressures. Although all samples show strongly tilted chains, the peak positions are different. While DPPC and **M4** exhibit an oblique chain lattice, for PA a centered rectangular unit cell of NN tilted chains is obtained.[34] The chain tilt amounts to 35 ± 1°, 21 ± 1°, and 20 ± 1° for DPPC, **M4**, and PA, respectively. The diffraction pattern of the mixture **M4** does not display signals at the positions found for DPPC or PA; hence, a complete miscibility has to be assumed. Therefore, the change in slope of the isotherms in mixtures up to 20% PA content should not be interpreted as the second-order phase transition of pure fatty acid; the change in slope is more likely a transition between two condensed phases of the mixture. For the isotherm of **M4**, this change in slope occurs at 27 mN/m. GIXD measurements at 25 mN/m reveal a tilted phase with NN tilt direction. At a higher pressure of 40 mN/m, a hexagonal phase with nontilted chains resulting from a second-order phase transition was observed. These findings are in agreement with the results from the Brewster angle microscopy experiments, showing low contrast at high pressures and high PA concentrations, which can now be explained by a uniform orientation of upright oriented molecules.

The Bragg peaks have been fitted using a Lorentzian model.[34,46] Assuming an exponential decay of the correlation as found in liquid crystals, the full width at half-maximum (fwhm) corresponds to the correlation length: $\xi = 2/\text{fwhm}(Q_{XY})$.[34] For the mixtures with tilted chains at low lateral pressures, the correlation length, ξ, shows remarkable differences in different directions. The (01), (10) reflections exhibit a comparable peak width which is larger than that observed for the (11) reflection. This difference leads to ratios of the correlation lengths in the three lattice directions from about 1/1/3 to 1/1/5. With decreasing tilt, the correlation perpendicular to the tilt direction decreases while the correlations in the tilt direction remain almost constant. Such an anisotropy of the correlations is also found in fatty acid and fatty alcohol monolayers,[39,47] Langmuir−Blodgett films on solid supports,[48−50] and smectic liquid crystalline phases.[51,52] Consequently, this feature points to comparable molecular mechanisms that might be responsible for phase transitions of layered systems.

This study indicates that PA induces changes in both the physicochemical parameters and structures of condensed DPPC/POPG mixed films at the air−water interface. The lipid−fatty acid interaction enables a close-packed, upright orientation, which is not found in the single-component systems. As PA concentration increases, the transition pressure toward upright orientation shifts to lower values and the lateral density is increased. Such a change in the short-range ordering of condensed domains could contribute to the improvement of lung surfactant replacements that is found on addition of PA.

Acknowledgment. F. Bringezu acknowledges financial support from the Deutsche Forschungsgemeinschaft (Emmy-Noether-Program Grant BR 1826/2-1). J.A.Z. and J.D. acknowledge financial support from NIH Grant HL-51177 and the University of California Tobacco Related Disease Research Program, Grants 8RT-0077 and 8DT-0171.

LA0103158

(46) Helm, C. A.; Möhwald, H.; Kjaer, K.; Als-Nielsen, J. *Biophys. J.* **1987**, *52*, 381−390.
(47) Majewski, J.; Popovitz-Biro, R.; Bouwman, W. G.; Kjaer, K.; Als-Nielsen, J.; Lahav, M.; Leiserovitz, L. *Chem.−Eur. J.* **1995**, *1*, 304−311.
(48) Tippmann-Krayer, P.; Kenn, R. M.; Mohwald, H. *Thin Solid Films* **1992**, *210/211*, 577−582.
(49) Sikes, H.; Schwartz, D. K. *Science* **1997**, *278*, 1604−1607.
(50) Schwartz, D. K. *Surf. Sci. Rep.* **1997**, *27*, 241−334.
(51) Brock, J. D.; Aharony, A.; Birgeneau, R. J.; Evans-Lutterodt, K. W.; Litster, J. D.; Horn, P. M.; Stephenson, G. B.; Tajbakhsh, A. R. *Phys. Rev. Lett.* **1986**, *57*, 98−101.
(52) Neundorf, M.; Diele, S.; Ernst, S.; Saito, S.; Demus, D.; Inukai, T.; Murashiro, K. *Ferroelectrics* **1993**, *147*, 95−108.